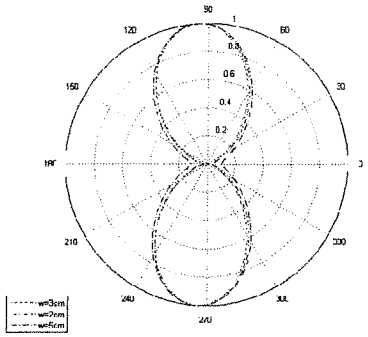

(a)

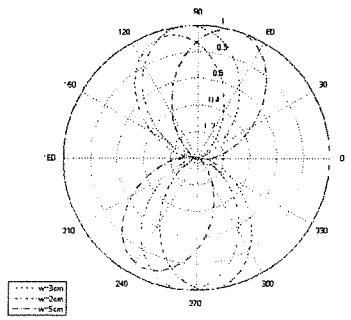

(b)

Figure 8: Radiation pattern of the monopole antenna mounted on the handset with $w = 3$ cm (—), $w = 2$ cm (---) and $w = 5$ cm (-.-.-); (a) in x-z plane ($\phi = 0$), (b) in y-z plane ($\phi = 90$).

5. CONCLUSION

The governing electrical field integral equation in time domain of a monopole antenna on a conducting box (a cellular handset) is solved by the method of moment in a wide range of operating frequencies. It is shown that the length and the width the handset have insignificant effects on its electromagnetic characteristics, but the height of the handset could slightly change the direction of the antenna main lobe. The position of the monopole on the handset top is shown to shift the position of the radiation pattern to the side which could be used to reduce the radiation on the user's head. In addition, it is shown that a radiating handset of dimensions less than $\lambda/4$ can be approximated by a single monopole wire antenna. This finding should simplify the solution of electromagnetic radiation due to a cellular phone in the vicinity of a dielectric medium such as human brain.

6. REFERENCES

[1] C. Johansen, JD. Boice et al, "Cellular telephones and cancer – a nationwide cohort study in Denmark", *J Natl Cancer Inst 93, pp.* 203-207, 2001.

[2] M. A. Jensen, Y. Rahmat-Samii, "EM interaction of handset antennas and a human in personal communications", in *Proc.* 1995 *IEEE*, vol. 83, no 1, pp. 7-17.

[3] O. P. Gandhi, G. Lazzi, C. M. Furse, "Electromagnetic absorption in the human head and neck for mobile telephones at 835 and 1900 MHz", *IEEE, MIT* vol. 44.10, Oct. 1996.

[4] K. S. Kunz and R. J. Luebbers, *The Finite-Difference Time-Domain Method in Electromagnetics,* Boca Raton, FL: CRC, 1993.

[5] A. Taflove, *Computational Electrodynamics: The Finite-Difference Time-Domain Method.* Dedham, MA: Artech House, 1995.

[6] R. Luebbers, L. Chen, T. Uno, S. Adachi, "FDTD calculation of radiation patterns, impedance, and gain for a monopole antenna on a conducting box", *IEEE trans. Ant. and Propagat.*, vol. 40, no 12, Dec. 1992.

[7] Li Yuying, Dong Tao, Xu Xiaowen, "Study of the Characteristics of a Portable Hanad-held phone Antenna by MoM", *in Proc.* 2000 *of the 3'rd International Conference on Microwave and Millimeter Wave Technology.*

[8] R. Sarraf, R. Moini, S. H. H. Sadeghi, "Analysis of electromagnetic fields due to a cellular phone handset, using the electric field integral equation method in time domain", *Proc.* 2003 *of 6's International Conference on Computational Methods in Electrical Engineering and Electromagnetics (ELECTROCOMP),* pp. 53-61.

[9] P. Bernardi, M.Cavagnaro, S. Pisa, and Em. Piuzzi, "Power absorption and temperature elevation in the human head by a dual-band monopole-helix antenna phone", *IEEE trans. Microwave Theory*, vol. 49, pp. 2539-2546, 2001.

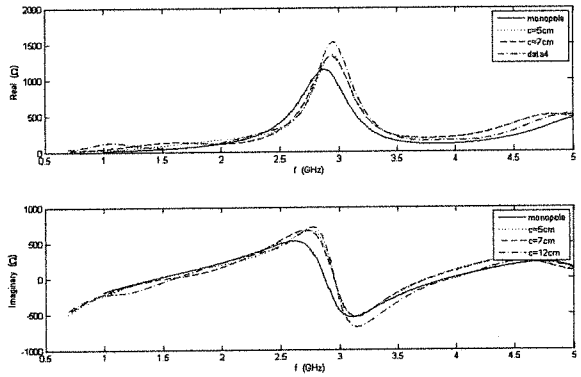

Figure 5: Input impedance of the monopole antenna without conducting box and with conducting box with various heights (---).

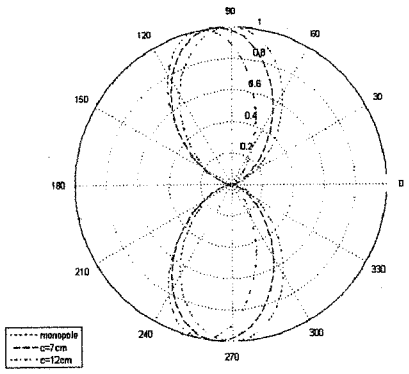

(a)

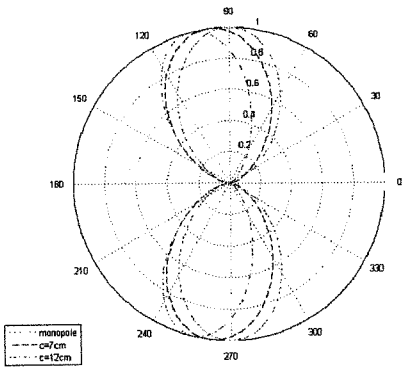

(b)

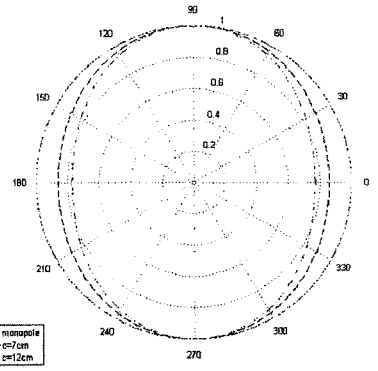

(c)

Figure 6: Radiation pattern of the monopole antenna (—), mounted on the handset with $c = 7$ cm (---), and mounted on the handset with $c = 12$ cm (-.-.-); (a) in y-z plane ($\phi = 90$), (b) in x-z plane ($\phi = 0$), and (c) in x-y plane ($\theta = 90$).

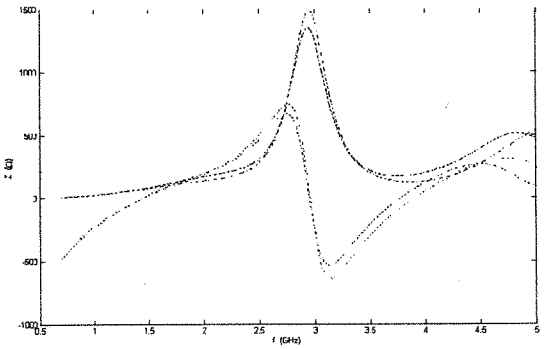

(a)

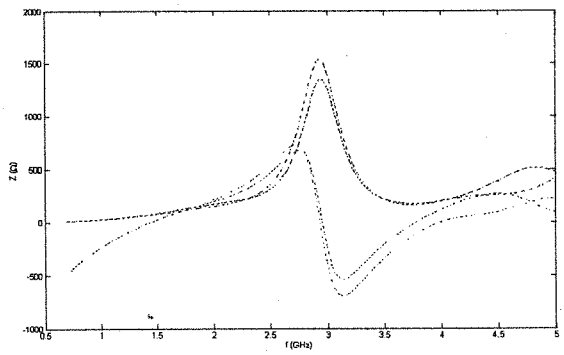

(b)

Figure 7: Input impedance of the monopole antenna with different box widths. (a) $b = 1$ cm (—), $b = 2$ cm (---). (b) $b = 6$ cm (—), $b = 7$ cm (---).

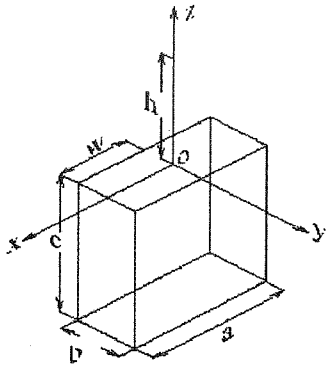

Figure 2: The geometric structure of the handset body together with its radiating monopole antenna.

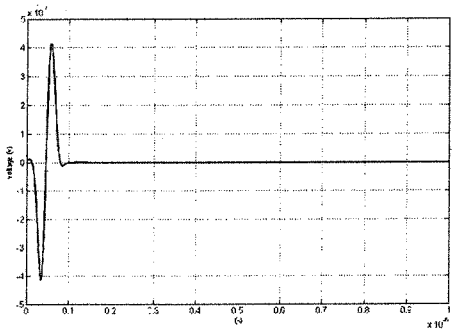

(a)

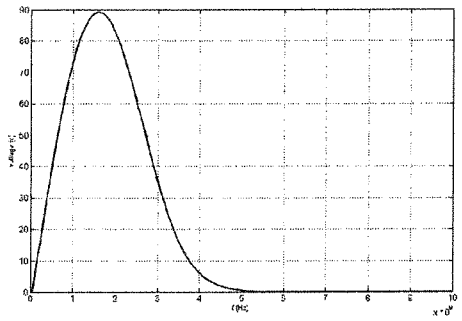

(b)

Figure 3: Source excitation voltage; (a) Time domain, (b) Frequency domain.

TABLE 1: PHYSICAL DIMENSIONS OF THE HANDSET BODY AND ITS MONOPOLE ANTENNA USED IN THE CASE STUDIES.

a = 6,7 cm	b = 1,2 cm	c = 5,7,12 cm
h = 5 cm	w = 3 cm	r = 0.1 mm

TABLE 2: PARAMETERS OF THE SOURCE EXCITATION VOLTAGE.

$t_{max}=4.58333 \times 10^{-10}$	$a_n=4.68131 \times 10^{9}$ 1/s
f_z=1500 MHz	

4. DISCUSSION

The validity of the proposed modeling is verified by comparing our simulated results with those reported by Luebbers, et al. [6]. Figure 4 shows the input impedance of the antenna when c = 5 cm, r = 0.5 mm and operating frequency varies from 0 to 5 GHz. As can be seen in this figure, for the practical range of operating frequency (i.e., f_z=0.7-2 GHz), the two results are in excellent agreement. Also, for larger values of f_z, our results qualitively follow the FD results although they tend to depart from each other. This discrepancy is believed to be due to the inherent incapability of the FD method for modeling wire structures, particularly for large operating frequencies [9].

Figure 5 depicts the variations of the real and imaginary parts of the input impedance versus operating frequency when c=5 cm, 7 cm and 12 cm. As can be seen, the handset body causes the antenna free-space resonant frequency to change from f_z = 1.5 GHz to 1450, 1470 and 1580 MHz. This is due to the induced current on the surface of the handset body, altering the free-space field distribution.

Next, we investigate the radiation pattern variations of the antenna in *xy*, *yz*, and *xz* planes as shown in Figure 6 (a), (b), and (c), respectively. An examination of Figure 6 demonstrates that the handset height has a slight effect on the antenna radiation pattern, particularly when compared with the case where the antenna is placed on an infinite planar perfect conductor. A further examination of Figure 6 demonstrates that when the handset height exceeds $\lambda/4$, the symmetry axis of the main lobe in the radiation pattern tends to depart from the antenna axis (i.e., *z*-axis).

Figure 7 (a) and (b) show the variations of the input impedance at different handset widths and lengths. It is shown that these variations have no significant effect on the input impedances in the working frequency range (i.e., 0.7-2 GHz.).

Figure 8 illustrates the impact of the monopole position (w) on the radiation pattern. It is observed that the position of the monopole antenna shifts the main lobe of the antenna to the side. This effect could be used to reduce the amount of the radiation reaching human brain which is considered to be the most harmful.

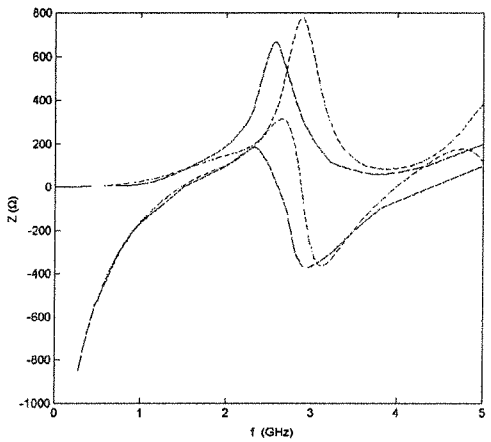

Figure 4: Computed input impedance of the monopole antenna mounted on the handset with height c = 5 cm (—) the proposed method, (---) the method given in [6].

tangential electric field at the conductor surface of equation (7) the electric field integral equation for thin conducting wires is obtained.

$$\mathbf{s}.\mathbf{E}^{A}(\mathbf{r},t)=\frac{\mu_0}{4\pi}\int_C[\frac{\mathbf{s}.\mathbf{s}'}{R}\frac{\partial}{\partial t'}I(s',t')+ c\frac{\mathbf{s}.\mathbf{R}}{R^2}\frac{\partial}{\partial s'}I(s',t')-c^2\frac{\mathbf{s}.\mathbf{R}}{R^3}q(s',t')] \quad (8)$$

$$\mathbf{r}\in C(\mathbf{r})+a(\mathbf{r})$$

where q can be expressed in terms of I as

$$q(s',t')=-\int_{-\infty}^{t'}\frac{\partial}{\partial s'}I(s',\tau)d\tau$$

and $a(\bar{r})$ denotes the wire radius at point $\bar{r}$. Since the integration path in equation (8) is along $C(\bar{r})$ while the wire radius displaces the field evaluation path, it is always true that R > 0 and the integral in equation (8) thus has no singularity. This displacement of the observation and source locations by the wire radius is the essence of the thin wire approximation.

To solve (8) by MoM, the first step is to divide the thin wire in to N_S elementary segment of length Δ_i. In addition, the time is divided into N_t equal step Δ_t. Next, a set of rectangular basis function is defined for expressing the known current in each of the segment.

$$I(s_0,t_0)=\sum_{i=1}^{N_S}\sum_{j=1}^{N_T}I_{ij}(s_i'',t_j'')U(s_i'')V(t_j'') \quad (9)$$

$$s_i''=s_0-s_i,\ t_i''=t_0-t_i$$

$$U\left(s_i''\right)=\begin{cases}1 & |s_i''|\le\Delta_i/2\\ 0 & \text{otherwise}\end{cases}$$
$$V\left(t_i''\right)=\begin{cases}1 & |t_i''|\le\Delta_i/2\\ 0 & \text{otherwise}\end{cases} \quad (10)$$

A second order polynomial representation is used to evaluate the current $I_{ij}(s_i'',t_j'')$ and the interpolation is chosen to be Lagrangian:

$$I_{ij}\left(s_i'',t_j''\right)=\sum_{l=-1}^{+1}\sum_{m=v}^{v+2}B_{ij}^{(l,m)}I_{i+1,j+1} \quad (11)$$

with

$$B_{ij}^{(l,m)}=\prod_{p=-1}^{+1}\prod_{q=v}^{v+2}\frac{(s_o-s_{i+p})(t_o-t_{j+q})}{(s_{i+1}-s_{i+p})(t_{j+m}-t_{j+q})} \quad (12)$$

$$\begin{cases}v=-1; & \Delta R=\dfrac{R}{c(t_j-t_{j-1})}>0.5\\ v=-2; & \Delta R<0.5\end{cases} \quad (13)$$

where $I_{i+1,j+m}$ is the current value at the center of the $(I+1)$ th space segment and the $(j+m)$ th time step.

The last step involves the selection of the test function in order to get a system of linear equations. The point matching method, based on Dirac distributions, is used, i.e.,

$$\begin{matrix}\delta(t-t_u) & \text{in the space}\\ \delta(t-t_v) & \text{in the time}\end{matrix} \quad (14)$$

Then we obtain the following system of equations where $(I_{i,v})$ is the unknown vector at every time step $v\Delta_t$.

$$(I_{iv})=(Z_{uv})^{-1}\{(e_{uv}^{a})-(e_{ux}^{d})\} \quad (15)$$

with

i=1,..., N_s ; u=1,..., N_s v=1,... N_T x=1, ..., v-1

where (Z_{iu}) is the matrix of the mutual interactions between the segments. This matrix has the advantage of being time independent.

3. Results

The theoretical model described above is used to compute the electromagnetic field intensity around the handset.

As shown in Figure 2, the handset body is approximated by a metallic box of dimensions of $a\times b\times c$. A monopole wire antenna of length h ($h=\lambda/4$) and radius r is placed at the top center of the handset body along the z-axis ($w=3$cm). It should be noted that since the technique is general, the model can be used for more complex the handset geometries as well.

To study the effect of the working frequency, we assume that the source is a modulated Gaussian pulse whose magnitude, $v(t)$ is defined as:

$$v(t)=\sin(2\pi f_z(t-t_{\max}))\exp(-a_n^2(t-t_{\max})^2) \quad (16)$$

where $t_{\max}$, a_n and f_z define the pulse shape. It should be noted that the Fourier transform of such a waveform is also a Gaussian function with a central frequency of f_z.

Table 1 lists the handset and antenna dimensions in our simulation. The parameters of the source excitation voltage are given in Table 2. Figure 3 shows the source waveform in time and frequency domains

manner in which the various terms in the final equation originate, it is used here.

It has been determined that integral equations of the magnetic type are generally more suitable to the treatment of solid surfaces. On the other hand, the electric-field integral equation is a better choice for the analysis of wire structures. Since the analysis of wire antennas and scatterers is interested the electric-field integral equation is chosen. While an equation based on the vector potential formulation would perhaps serve as well for some problems, it appears from a practical viewpoint that numerical solution of the electric-field equation is more conveniently obtained and is applicable without reformulation to a wider class of problem.

The time-dependent Maxwell's equations are the starting point of derivation:

$$\nabla\times\mathbf{E}=-\mu_0\frac{\partial}{\partial t}\mathbf{H}$$

$$\nabla\times\mathbf{H}=\varepsilon_0\frac{\partial}{\partial t}\mathbf{E}+\mathbf{J} \qquad (1)$$

$$\nabla.\mathbf{J}+\frac{\partial}{\partial t}\rho=0 \qquad \nabla.\mathbf{H}=0$$

where μ_0 and ε_0 represent the permeability and permittivity of free space, $\mathbf{E}$ and $\mathbf{H}$ are the electric and magnetic fields, and $\mathbf{J}$ and ρ are the volume current and charge densities, respectively.

The required integral equation may be derived by the vector Green's identity combined with (1). This equation relates $\mathbf{J}$ and $\mathbf{E}$ on the surface of considered structure. It is assumed that the structure is wire like with a circular cross section small compared with the wavelength of the highest significant frequency component of the excitation spectrum.

The filamentary current density $\mathbf{I}(\mathbf{r},t)$ flows on the path $C(\mathbf{r})$ along which the length variable is s (Figure 1). It produces electric field given below:

$$\mathbf{E}(\mathbf{r},t)=-\nabla\Phi(\mathbf{r},t)-\frac{\partial}{\partial t}\mathbf{A}(\mathbf{r},t) \qquad (2)$$

where

$$\mathbf{A}(\mathbf{r},t)=\frac{\mu_0}{4\pi}\int_C\frac{\mathbf{I}(\mathbf{r},t-R/v)}{R}ds' \qquad (3)$$

and

$$\mathbf{A}(\mathbf{r},t)=\frac{\mu_0}{4\pi}\int_C\frac{\mathbf{I}(\mathbf{r},t-R/v)}{R}ds' \qquad (4)$$

where $\mathbf{s}=\mathbf{s}(\mathbf{r})$, $\mathbf{s}'=\mathbf{s}(\mathbf{r}')$, $\mathbf{ds}'=\mathbf{ds}(\bar{\mathbf{r}}')$, $R=|\mathbf{R}|=|\mathbf{r}-\mathbf{r}'|$ and the unprimed coordinates $\mathbf{r}$ and t denote the observation point location and the primed coordinates $\mathbf{r}'$ and $t'=t-R/c$ the source location. The differential operators in (2) are with respect to the observation coordinate.

If $\mathbf{s}=\mathbf{s}(\mathbf{r})$ and $\mathbf{s}'=\mathbf{s}(\mathbf{r}')$ are the unit tangential vectors to $C(\mathbf{r})$ at $\mathbf{r}$ and $\mathbf{r}'$, then the required terms in (2) can be written

$$\frac{\partial}{\partial t}\mathbf{A}(\mathbf{r},t)=\frac{\mu_0}{4\pi}\int_C\frac{\mathbf{s}'}{R}\frac{\partial}{\partial t'}I(\mathbf{r}',t')ds' \qquad (5)$$

and

$$\nabla\Phi(\mathbf{r},t)=\frac{1}{4\pi\varepsilon_0}\int_C\left[-q(\mathbf{r}',t')\frac{\mathbf{R}}{R^3}+\frac{\mathbf{R}}{R^2c}\frac{\partial}{\partial s'}I(\mathbf{r}',t')\right]ds' \qquad (6)$$

where the following has been used:

$$\nabla q(r',t')=\frac{\partial}{\partial s'}I(r',t')\frac{\mathbf{R}}{R.c}$$

And

$$\frac{\partial}{\partial s'}I(\bar{r}',t')=-\frac{\partial}{\partial t'}q(r',t').$$

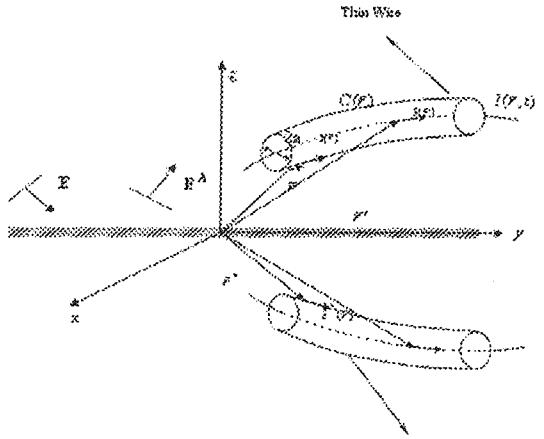

Figure 1: Thin wire geometry.

Upon noting that $I(r',t')\equiv I(s',t')$ and $q(\bar{r}',t')\equiv q(s',t')$ and combining (5) and (6) with (2) the integral equation form of the electric field due to a filamentary current is derived:

$$\mathbf{E}(\mathbf{r},t)=-\frac{\mu_0}{4\pi}\int_C[\frac{\mathbf{s}'}{R}\frac{\partial}{\partial t'}I(s',t')+c\frac{\mathbf{R}}{R^2}\frac{\partial}{\partial s'}I(s',t')-c^2\frac{\mathbf{R}}{R^3}q(s',t')]ds' \qquad (7)$$

This equation for all space and time except the source region is valid. In fact the source region is a conductor of nonzero cross section. Applying the standard thin wire approach it is assumed that $I(s',t')$ and $q(s',t')$ are confined to the conductor axis and that the boundary condition on the tangential electric field at the conductor surface is known. For a perfect conductor $\mathbf{s}.(\mathbf{E}+\mathbf{E}^{\mathbf{A}})=0$. $\mathbf{E}^{\mathbf{A}}$ and $\mathbf{E}$ are the applied and generated fields respectively. By applying the boundary condition on the

Calculation of EM Characteristics of a Cellular Phone Handset by Time-Domain MoM

R. Sarraf;[i] R. Moini;[ii] S. H. H. Sadeghi[iii]; and A. Farschtschi[iv]

ABSTRACT

The effect of cellular phone handset dimensions on radiation pattern, impedance and resonance frequency is investigated. The hand-set body is modeled by an appropriate three-dimensional wire-grid structure with a $\lambda/4$ monopole antenna as its radiating source. The governing electric field integral equation (EFIE) is solved in the time domain, using the method of moments (MoM). The validity of the model is demonstrated by comparing the wide-band results of the antenna input impedance with those available in the literature. It is shown that at current operating frequencies, a regular handset dimensions has minimal effect on the antenna radiation pattern and impedance, and hence modeling of a handset by its antenna (monopole) is sufficient.

KEYWORDS

Method of Moments, EFIE, Time-Domain, Cellular Phone, Input Impedance, Radiation Pattern

1. INTRODUCTION

In the last decade, there has been an enormous growth in the wireless communication usage and there are more than two thousand millions cellular users are reported at the end of 2005 [1]. Biological effects of a handset close range radiation on human body and its medical consequences are of great concern. It is desired to reduce the negative impact of field on the brain which is most susceptible of all body organs to this problem. Therefore, we need a model showing the radiated field of an antenna in the presence of the cellular phone main body. The trend for small size phones necessitates the study of the antenna pattern with different handset body dimensions.

Due to irregular shape of a handset, numerical methods are best suited for analysis of electromagnetic fields. The Finite Element Method (FEM), the Finite Difference Method (FDM) and the Method of Moment (MoM) are most widely utilized in the literature. Recently, the FDM in time domain (FDTD) has been preferred by many researchers [2-5]. In this method, the coupled Maxwell's equations in differential form are solved in both space and time. The FDTD method is not efficient for analyzing metallic structures such as antennas due to its large computer time and memory requirements [6]. In contrast, the MoM has been efficiently used for analyzing thin-wire structures [7, 8].

Here, we use the MoM for analyzing electromagnetic field distributions around a radiating cellular phone handset. In particular, we focus on how the physical dimensions of the handset can affect the radiation pattern, resonance frequency and input impedance of the antenna.

Section 2 presents the theoretical model of the problem and describes how the governing EFIE is solved using the method of moment in time domain. Section 3 discusses the simulation results for a small telephone handset excited by a monopole antenna.

2. THEORY

Several methods have been introduced for developing time-dependent integral equations. One obvious approach is the Fourier transform of the frequency domain relations. In this approach, one might return to the time-dependent Maxwell's equations and proceed to derive directly in the time domain the particular equation type of interest. Since this approach will generally show in a clearer way the

i R. Sarraf is with the Department of Electrical Engineering, Amirkabir University of Technology, Tehran, Iran (e-mail: sarraf@aut.ac.ir).

ii R. Moini is with the Department of Electrical Engineering, Amirkabir University of Technology, Tehran, Iran (e-mail: moini@aut.ac.ir).

iii S. H. H. Sadeghi is with the Department of Electrical Engineering, Amirkabir University of Technology, Tehran, Iran (e-mail: sadeghi@aut.ac.ir).

iv A. Farschtschi is with the Faculty of Electronic and Information, Technical University of Chemnitz, Chemnitz, Germany (e-mail: LATE@e-technik.tu-chemnitz.de).